Rapid Communication *J. Biochem.* **128**, 349–354 (2000)

Crystal Structure of the Pyridoxal 5′-phosphate Dependent L-Methionine γ-Lyase from *Pseudomonas putida*

Hiroyuki Motoshima,[*] Kenji Inagaki,[†,1] Takashi Kumasaka,[*] Makio Furuichi,[*] Hiroyuki Inoue,[†] Takashi Tamura,[†] Nobuyoshi Esaki,[‡] Kenji Soda,[§] Nobuo Tanaka,[‖] Masaki Yamamoto,[*] and Hidehiko Tanaka[†]

[*]RIKEN Harima Institute, 1-1-1 Kouto, Mikazuki, Sayo-gun, Hyogo 679-5148; [†]Department of Bioresources Chemistry, Faculty of Agriculture, Okayama University, 1-1-1 Tsushima-naka, Okayama, Okayama 700-8530; [‡]Institute for Chemical Research, Kyoto University, Uji, Kyoto 611-0011; [§]Department of Biotechnology, Faculty of Engineering, Kansai University, 3-3-35 Yamate-cho, Suita, Osaka 564-8680; and [‖]Graduate School of Bioscience and Biotechnology, Tokyo Institute of Technology, 4259 Nagatsuta, Midori-ku, Yokohama, Kanagawa 226-8501

Received May 30, 2000; accepted July 6, 2000

L-Methionine γ-lyase (MGL) catalyzes the pyridoxal 5′-phosphate (PLP) dependent α,γ-elimination of L-methionine. We have determined two crystal structures of MGL from *Pseudomonas putida* using MAD (multiwavelength anomalous diffraction) and molecular replacement methods. The structures have been refined to an *R*-factor of 21.1% at 2.0 and 1.7Å resolution using synchrotron radiation diffraction data. A homotetramer with 222 symmetry is built up by non-crystallographic symmetry. Two monomers associate to build the active dimer. The spatial fold of subunits, with three functionally distinct domains and their quarternary arrangement, is similar to those of L-cystathionine β-lyase and L-cystathionine γ-synthase from *Escherichia coli*.

Key words: crystal structure, MAD, L-methionine γ-lyase, PLP enzyme, *Pseudomonas putida*.

L-Methionine γ-lyase (MGL) [EC 4.4.1.11] is a PLP enzyme that catalyzes α,γ-elimination of L-methionine to α-ketobutyrate, methanethiol, and ammonia, and γ-replacement of L-methionine and various thiols. MGL has only been found in several microorganisms such as *Pseudomonas* (MGL_Pp), *Aeromonas*, and *Clostridium*, *i.e.* not in yeast, plants, or mammals (*1*). Structurally, the enzyme is related to other enzymes involved in the metabolism, *via* the transsulfuration pathways, of L-cysteine and L-homocysteine, that together comprise the γ-family of PLP-dependent enzymes (*2*). Comparison of the sequences of MGL_Pp, and other α,γ-elimination and γ-replacement PLP enzymes is shown in Fig. 1. We found sequence similarities between MGL_Pp and the following enzymes: L-cystathionine β-lyase from *Escherichia coli* (CBL_Ec) (25%) (*3*), L-cystathionine γ-synthase from *E. coli* (CGS_Ec) (36%) (*4*), and two L-methionine γ-lyases from *Trichomonas vaginalis* (MGL1_Tv) (44%), (MGL2_Tv) (45%) (*5*). These enzymes consist of three domains, which are the N-terminal domain (blue), large PLP binding domain (green), and C-terminal domain (red) shown in Fig. 1. Their secondary structure (sec. struc.) elements are denoted by cylinders (α-helices) and arrows (β-strands). These enzymes catalyze γ-elimination or γ-replacement, and also β-elimination, β-replacement reactions with sulfur-containing amino acids. The structural information available for members of the γ-family was limited until the crystal structures of CBL from *E. coli* (*6*), and CGS from *E. coli* (*7*) and *Nicotiana tabacum* (*8*) were solved recently.

MGL_Pp has been characterized in some detail at the biochemical level (*1*). This enzyme is encoded by the *mdeA* gene, and cloning and expression of the *mdeA* gene was previously reported (*9*). The enzyme forms a homotetramer. Each monomer consists of 398 amino acids (M_r 42,626) and contains one PLP molecule as a cofactor, which is covalently linked to the ε-amino group of Lys211 (*10*). We have studied the catalytic mechanism of the enzyme using L-vinylglycine (*11*), and the mechanism of inactivation by analogues (*12*).

Studies of the antitumor efficacy of MGL *in vitro* and *in vivo* toward human tumors xenografted into nude mice demonstrated that all types of human tumors tested, including lung, colon, kidney, brain, prostate, and melanoma ones, were sensitive to MGL (*13*, *14*). In contrast, normal cells were insensitive to MGL *in vitro* and, correspondingly, no toxicity was detected *in vivo* with the effective doses. These data suggested that MGL could be a new protein medicine. However, the crystal structure of MGL has not been solved. In this paper, we report two types of crystal structures of MGL_Pp at 2.0 and 1.7 Å resolution.

MGL_Pp was purified from *Pseudomonas putida* as described previously (*15*). Crystallization of the enzyme was performed by the hanging-drop vapor-diffusion method, with equilibration against a reservoir solution containing 15% PEG6000, 250 mM NaCl, 200 mM MES-NaOH (pH 6.5), 0.5 mM PLP, and 0.5% 2-mercaptoethanol. A 4-μl drop comprising equal volumes of the reservoir solution and a solution of 10–20 mg/ml protein in 20 mM sodium phosphate (pH 7.2), 0.5 mM PLP, and 0.5% 2-mercaptoeth-

[1] To whom correspondence should be addressed.

Abbreviations: MGL, L-methionine γ-lyase; CBL, L-cystathionine β-lyase; CGS, L-cystathionine γ-synthase; PLP, pyridoxal 5′-phosphate; MAD, multiwavelength anomalous diffraction; MES, 2-morpholinoethanesulfonic acid; PEG, polyethyleneglycol.

anol was kept at room temperature. Crystals (Crystal I) were grown within one week to a size of up to 0.3 × 0.3 × 0.2 mm^3. The crystals were soaked in a cryoprotectant (reservoir buffer supplemented with 20% glycerol), and then mounted in the loop and flash-cooled to 100K using a Cryostream Cooler (Oxford Cryosystems). MAD data for a Pb derivative crystal and native data were collected with the trichromatic concept at RIKEN beamline I (BL45XU) in SPring-8 station (Mikazuki, Hyogo) using a Rigaku R-AXIS IV imaging-plate system. The space group of Crystal I was tetragonal, $P4_32_12$. The cell dimensions of the Pb derivative and the native crystals are shown in Tables I and II. Crystal I contains four monomers in the asymmetric unit, with a solvent content of 56% and a V_M value of 2.79 Å^3/Da, which is in the range for most common protein crystals (*16*). Three data sets for the Pb derivative crystal were collected using wavelengths on and around the Pb L_{III} absorption edge, and a remote point. All data were processed and scaled with the programs DENZO and SCALEPACK (*17*). The intensity measurement results are shown in Tables I and II. Heavy-atom parameter refinement and phase calculation were carried out using the program SOLVE (*18*). Phase improvement by solvent flattening, histogram matching, and non-crystallographic symmetry averaging was carried out using the program DM (*19*). The atomic model was built using the graphic program TURBO-FRODO (*20*). The model was refined against the native data for MGL_Pp with the program CNS (*21*) using positional and *B*-factor refinement, followed by simulated annealing refinement with experimental phases. Parts of the model, which were initially difficult to trace, were fitted successively to F_{obs}–F_{calc} and $2F_{obs}$–F_{calc} maps. The final stage of refinement did not involve experimental phases and non-crystallographic symmetry strict or restrain. The final model has an *R*-factor of 21.1% between 500 and 2.0 Å.

Crystallization of MGL (Crystal II) was performed under the same conditions as for Crystal I except that the reservoir solution contained 15% PEG6000, 250 mM $(NH_4)_2SO_4$, 200 mM Tris-HCl (pH 8.5), 0.5 mM PLP, and 0.5% 2-mercaptoethanol. Crystal II was grown within one week to a size of up to 0.2 × 0.2 × 0.2 mm^3. Diffraction data for a native crystal were collected by means of synchrotron radiation at SPring-8. The space group of Crystal II was triclinic, *P*1. The cell dimensions of Crystal II are shown in Table II. Crystal II also contains four monomers in the asymmetric unit. The results of intensity measurement of Crystal II are shown in Table II. Structure solution by molecular replacement techniques was performed using the program package AMoRe (*22*). The coordinates of the homotetramer in Crystal I were used as a search model. The model of Crystal II was built using the methods used for Crystal I without experimental phases. The final model has an *R*-factor of 21.1% between 500 and 1.7 Å. The coordinates of Crystal I and Crystal II have been deposited in the Protein Data Bank under ID codes 1GC2 and 1GC0, respectively.

The model was kept close to standard geometry throughout the refinement. The mean positional errors of the atoms, as estimated from a Lauzatti plot (*23*) are 0.26 (Crystal I) and 0.20 (Crystal II) Å. The quality of the final models is summarized in Table I. The main chain dihedral angles are all well defined, and the values of all non-glycine residues are within energetically allowed regions (*24*) except for that of Thr191. For Thr191 the electron density is well defined.

Like CBL and CGS, each MGL subunit is divided into three domains, which are the N-terminal domain (blue), large PLP binding domain (green), and C-terminal domain

TABLE II. **Data collection and refinement statistics of two crystals.**

Crystal type	Crystal I	Crystal II
Space group	$P4_32_12$	*P*1
Cell parameters (Å)	$a=b=133.56$	$a=72.86$
		$b=81.03$
	$c=213.77$	$c=81.28$
	($\alpha=\beta=\gamma=90$)	$\alpha=72.86$
		$\beta=63.17$
		$\gamma=63.38$
Wavelength (Å)	1.0000	1.0200
Resolution (Å)	2.0	1.7
Observations	1,016,993	263,490
Independents	130,168	144,898
$I/\sigma(I)$	9.9	28.5
Completeness (%)	99.7	90.8
R_{merge} (%)	7.9	3.7
R-factor (%)	21.1	21.1
R_{free}-factor (%)	24.3	23.8
Number of non-hydrogen atoms	11,653	10,795
R.M.S deviations from ideality		
Bond length (Å)	0.006	0.005
Angles (°)	1.260	1.237
Dihedral angles (°)	22.544	22.130
Improper angles (°)	0.713	0.720

TABLE I. **Data collection and phasing statistics of derivative Crystal I.**

Wavelength (Å)	1.0025 (remote)	0.9485 (edge)	0.9503 (peak)
Cell parameters (Å)		$a=b=133.47$	
		$c=213.32$	
Space group		$P4_32_12$	
Anomalous atoms		4Pb/asymmetric unit	
M.W.		43 kDa/monomer	
Resolution (Å)	2.5	2.5	2.5
Observations	524,382	479,057	482,158
Independents	66,031	65,803	65,807
$I/\sigma(I)$	9.5	9.1	8.1
Completeness (%)	98.1	97.7	97.7
R_{merge} (%)	8.0	8.3	9.3
Z-score		27.2	
Figure of merit		0.28	
Figure of merit (after DM)		0.89	

(red) shown in Fig. 1. Their secondary structure (sec. struc.) elements are denoted by cylinders (α-helices) and arrows (β-strands). The active site residues of MGL_Pp are indicated by arrows. Each subunit has an extended N-terminal domain (residual 1–63) composed of helix 1 and a long loop structure comprising 46 residues. The large PLP binding domain (residual 64–262) comprises an open, mainly parallel, seven strand β-sheet (β-strands a, b, c, d, e, f, and g with directions +, −, +, +, +, +, and +, respectively), all cross-overs being right-handed. The β-sheet structure is sandwiched with eight α-helices (2 to 9). Helices 2, 6, 7 and 8 are located on one side of the β-sheet and shield it from the solvent, and helices 3, 4, 5, and 9, are located on the other side and comprise the interdomain interface. Short helices 5, 6, and 8 exhibit the hydrogen bonding pattern typical of 3_{10} helices. PLP is covalently attached to Lys211

Fig. 1. **Sequence alignment of MGL_Pp and other PLP-dependent enzymes of the γ-family based on the crystal structures.** Abbreviations used: CBL_Ec, L-cystathionine β-lyase of *E. coli*; CGS_Ec, L-cystathionine γ-synthase of *E. coli*; CGL_Hs, L-cystathionine γ-lyase of human; MGL1_Tv and MGL2_Tv, L-methionine γ-lyases of *Trichomonas vaginalis*; MGL_Pp, L-methionine γ-lyase of *Pseudomonas putida*. Conserved residues are shown in red, and homologous ones in yellow. Secondary structure (sec. struc.) elements are shown as cylinders (α-helices) and arrows (β-strands). Active site residues of MGL_Pp are indicated by arrows. The figure was produced using the program ALSCRIPT (*27*).

(*10*) and is located near the N-terminus of helix 3, and the C-termini of strands d, e, and f. The central part of the C-terminal domain (residual 263–398) is a five strand, mainly antiparallel β-sheet. Cross-overs are right-handed, and helices 12, 13, 14, 15, and 16 are all located on the solvent-accessible side of the β-sheet.

Continuous densities were visible in $2F_o$–F_c maps contoured at 1.2σ, except for the 6 N-terminal residues (residual 1–6), and the region between the N-terminal domain and the PLP-binding domain (residual 42–63) in Crystal I, and for the 6 N-terminal residues (residual 1–6), the region between the N-terminal domain and the PLP-binding domain (residual 42–63), and the C-terminal domain (residual 292–309) in Crystal II. The side chains of some residues on the surface of the molecules (residual 355–365) in Crystal I and (residual 110–119) in Crystal II exhibited weak or no electron density.

MGL_Pp is known to exist as a homotetramer in solution (*15*), and this quaternary structure is observed in the crystal structures. Figure 2a shows a ribbon model of the homotetramer (yellow, blue, green, and red denote each monomer). This model with 222 symmetry is built up by non-crystallographic symmetry. The molecules indicated by the sticks and balls in the ribbon model are PLP. The dimensions of the tetramer are about 90 Å × 80 Å × 80 Å. Despite their crystallographic independence, any pair of monomers (AB, AC, AD, BC, BD, and CD) can be superim-

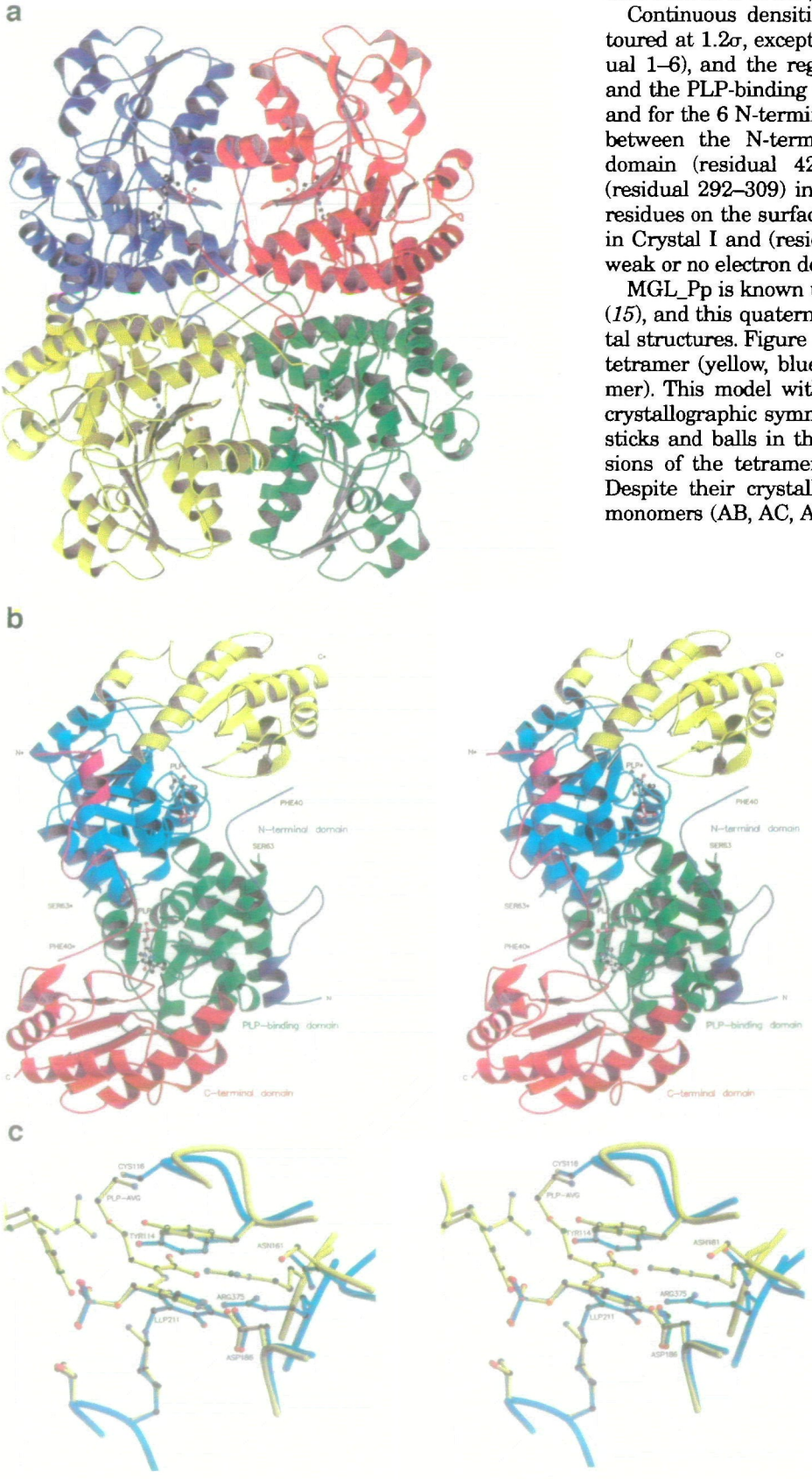

Fig. 2. Three-dimensional structure of MGL_Pp. (a) Ribbon model of the homotetramer built up as a dimer of active dimers, resulting in an overall 222 symmetry. (b) Stereo view of the ribbon model of active dimers. The location of the PLP-binding site is shown as a ball-and-stick model. Another monomer is labeled with an asterisk (*). (c) Comparison of the active site structures of MGL_Pp (blue) and CBL_Ec with aminoethoxylvinylglycine (AVG) (yellow). The residual labels are given for MGL_Pp.

TABLE III. **The correlated residues in CBL_Ec and CGS_Ec of the ζ-carboxyl and ζ-amino groups of L-cystathionine, and the residues in MGL_Pp corresponding to the sequences of these residues.**

L-Cystathionine	ζ-Carboxyl group	ζ-Amino group	
CBL_Ec	Arg59*	Glu235*	
MGL_Pp	Ile62*	Leu236*	
CGS_Ec	Arg49*	Asp45*	Glu325
MGL_Pp	Ile62*	Phe58*	Val339

Another monomer of the active dimer is labeled with an asterisk (*).

posed with root-mean-square deviations of 0.32, 0.27, 0.27, 0.25, 0.34, and 0.29 Å (Crystal I), 0.14, 0.23, 0.11, 0.11, 0.12, and 0.14 Å (Crystal II), 0.66 Å (as of Crystals I and II), respectively. Moreover, MGL, CBL and CGS can be superimposed with root-mean-square deviations of 1.32 (MGL vs CBL) and 1.34 (MGL vs CGS). Their quarternary arrangements were very similar. Two monomers associate tightly to build the active dimer, as shown in Fig. 2b. The location of the PLP-binding site is shown in the ball-and-stick presentation. Another monomer is labeled with an asterisk (*). The N-terminal domain protrudes from the core domain of the monomer and clamps the other core domain to its respective partner monomer. The two active sites are separated by about 20 Å. For several enzymes of the γ-family, evidence has been obtained that only one active site per dimer is actually operating or being inhibited by mechanism-based inactivators (*12*). The contacted N-terminal regions were significantly more disordered. The more flexible active site environment could lead to easier acceptance of a substrate by way of an induced fit mechanism (*7*). Because the average *B* value of MGL_Pp is larger than that of CBL_Ec, *i.e.* by about 10 Å^2, it is considered that the conformation of the contacted N-terminal regions (residual 42–63) could not be modeled in MGL_Pp. The MGL_Pp cannot catalyze L-cystathionine and L-norleucine. Although L-norleucine can inhibit the elimination reaction for L-methionine, L-cystathionine can not inhibit it. There are correlated residues (residual Arg59 and Glu235 in CBL_Ec, and Arg49, Asp45, and Glu325 in CGS_Ec) with ζ-carboxyl and ζ-amino groups of L-cystathionine. These residues are compared with the corresponding residues (residual Ile62 and Leu236, Ile62, Phe58, and Val339) in MGL_Pp (Table III). Although these correlated residues were all hydrophilic amino acids in CBL and CGS, they were all hydrophobic ones in MGL_Pp. It is considered that L-cystathionine can not bind the active site of MGL_Pp. However, it can be supported that MGL_Pp catalyzes the γ-addition of L-vinylglycine, and the γ-replacement reaction of L-methionine and alkanthiols (*11*).

Cys116 of MGL_Pp was proposed to be a nucleophilic residue for an enzymatically activated 3,4-allenic intermediate of these inactivators, and also modified and identified with *N*-(bromoacetyl)pyridoxamine phosphate (a cofactor analogous affinity-labeling agent), 2-nitro-5-thiocyanobenzoate (NTCB), and indoacetate (*10*). Kinetic analysis of MGL_Pp Cys-cyannilated with NTCB also revealed that the affinity of the enzyme for the substrates was greatly decreased (*25*). Although Cys116 was not conserved in other γ-family enzymes, the region around Cys116 is highly conserved and Tyr114 is common in all known sequences of γ-family enzymes (Fig. 1). As a result of an attempt to define the role of Tyr114 and Cys116, it was found that Tyr114 but not Cys116 plays a role in the catalytic activity (*26*). The structure of MGL_Pp supports this evidence. Compared the structure of the PLP-binding region in CBL_Ec and inhibitor (L-aminoethoxylvinylglycine, AVG) complex with that in MGL_Pp, Tyr114-OH in MGL_Pp was more closely the C_γ of the inhibitor than Cys116-SH in MGL_Pp. Figure 2c shows a comparison of the active site structures of MGL_Pp (blue) and CBL_Ec with AVG (yellow). The residual labels are given for MGL_Pp.

In summary, MGL_Pp is crystallized as an α_4 tetramer with subunits related by non-crystallographic 222 symmetry. The spatial fold of subunits, with three functionally distinct domains and their quarternary arrangement, is similar to those of CBL and CBS. The N-terminal region (residual 42–63), which plays a role in substrate recognition, is very flexible in MGL_Pp. To reveal the catalytic mechanism of MGL_Pp in more detail, it is necessary to analyze the crystal structures of the active site mutated enzymes and the substrate analogue-enzyme complexes.

We wish to thank Ms. Fumiko Numayama of the Graduate School of Bioscience and Biotechnology, Tokyo Institute of Technology, for her help in the crystallization of L-methionine γ-lyase.

REFERENCES

1. Esaki, N. and Soda, K. (1987) L-Methionine γ-lyase from *Pseudomonas putida* and *Aeromonas* in *Methods in Enzymology* (Jakoby, W.B. and Griffith, O.W., eds.) Vol. 143, pp. 459–465, Academic Press, New York
2. Alexander, F.W., Sandmeier, E., Metha, P.K., and Christen, P. (1994) Evolutionary relationships among pyridoxal 5′-phosphate-dependent enzymes. Regio-specific α, β and γ families. *Eur. J. Biochem.* **219**, 953–960
3. Belfaiza, J., Parsot, C., Martel, A., Boutheir De La Tour, C., Margarita, D., Chohen, G.N., and Saint-Girons, I. (1986) Evolution in biosynthetic pathways: Two enzymes catalyzing consecutive steps in methionine biosynthesis originate from a common ancestor and possess a similar regulatory region. *Proc. Natl. Acad. Sci. USA* **83**, 867–871
4. Duchange, N., Zakin, M.M., Ferrara, P., Saint-Girons, I., Park, I., Tran, S.V., Py, M.C., and Cohen, G.N. (1983) Structure of the *metJBLF* cluster in *E. coli* K12. Sequence of the *metB* structural gene and the 5′- and 3′-flanking regions of the *metBL* operon. *J. Biol. Chem.* **258**, 14868–14871
5. MacKie, A.E., Edlind, T., Walker, J., Mottram, J.C., and Coombs, G.H. (1998) The primitive Protozoon *Trichomonas vaginalis* contains two methionine γ-lyase genes that encode members of the γ-family of pyridoxal 5′-phosphate-dependent enzymes. *J. Biol. Chem.* **273**, 5549–5556
6. Clausen, T., Huber, R., Laber, B., Pohlenz, H., and Messerchmidt, A. (1996) Crystal structure of the pyridoxal 5′-phosphate dependent cystathionine β-lyase from *E. coli* at 1.83 Å. *J. Mol. Biol.* **262**, 202–224
7. Clausen, T., Huber, R., Prade, L., Wahl, M.C., and Messerchmidt, A. (1998) Crystal structure of cystathionine γ-synthase from *E. coli* at 1.5 Å resolution. *EMBO J.* **17**, 6827–6838
8. Steeghorn, C., Messerchmidt, A., Laber, B., Streber, W., Huber, R., and Clausen, T. (1999) The crystal structure cystathionine γ-synthase from *Nicotiana tabacum* reveals its substrate and reaction specificity. *J. Mol. Biol.* **290**, 983–996
9. Inoue, H., Inagaki, K., Sugimoto, M., Esaki, N., Soda, K., and Tanaka, H. (1995) Structural analysis of the L-methionine γ-lyase gene from *Pseudomonas putida*. *J. Biochem.* **117**, 1120–1125
10. Nakayama, T., Esaki, N., Tanaka, H., and Soda, K. (1988) Specific labeling of the essential cysteine residue of L-methionine gamma-lyase with a cofactor analogue, *N*-(bromoacetyl)pyri-

doxamine phosphate. *Biochemistry* **27**, 1587–1591
11. Esaki, N., Suzuki, T., Tanaka, H., Soda, K., and Rando, R.R. (1977) Deamination and γ-addition reactions of vinylglycine by L-methionine γ-lyase. *FEBS Lett.* **84**, 309–312
12. Jonston, M., Jankowski, D., Marcotte, P., Tanaka, H., Esaki, N., Soda, K., and Walsh, C. (1979) Suicide inactivation of bacterial cystathionine γ-synthase and methionine γ-lyase during processing of L-proparglycine. *Biochemistry* **18**, 4690–4701
13. Tan, Y., Xu, M., Tan, X., Tan, X., Wang, X., Saikawa, Y., Nagahama, T., Sun, X., Lenz, M., and Hoffman, R.M. (1997) Overexpression and large-scale production of recombinant L-methionine-α-deamino-γ-mercaptomethane-lyase for novel anticancer therapy. *Protein Exp. Purif.* **9**, 233–245
14. Tan, Y., Sun, X., Xu, M., Tan, X., Han, Q., Miljkovic, D.A., Yang, M., and Hoffman, R.M. (1998) Polyethylene glycol conjugation of recombinant methioninase for cancer therapy. *Protein Exp. Purif.* **12**, 45–52
15. Nakayama, T., Esaki, N., Sugie, K., Beresov, T.T., Tanaka, H., and Soda, K. (1984) Purification of bacterial L-methionine γ-lyase. *Anal. Biochem.* **138**, 421–424
16. Matthews, B.W. (1968) Solvent content of protein crystals. *J. Mol. Biol.* **33**, 491–497
17. Otwiniski, Z. and Minor, W. (1997) Processing X-ray diffraction data collected in oscillation mode in *Methods in Enzymology* (Carter, C.W. Jr. and Sweet, R.M., eds.) Vol. 276, pp. 307–326, Academic Press, New York
18. Terwilliger, T.C. and Berendzen, J. (1999) Automated structure solution for MIR and MAD. *Acta Crystallogr.* **D55**, 849–861
19. Collaborative Computational Project, Number 4 (1994) The CCP4 suite: Program for protein crystallography. *Acta Crystallogr.* **D50**, 760–763
20. Roussel, A., Fontecilla-Camps, J.C., and Cambillau, C. (1990) TURBO-FRODO: A new program for protein crystallography and modeling. Bordeaux, France: XV IUCr Congess
21. Brunger, A.T., Adams, P.D., Clore, G.M., DeLano, W.L., Gros, P., Grosse-Kunstleve, R.W., Jiang, J.S., Kuszewski, J., Nilges, M., Pannu, N.S., Read, R.J., Rice, L.M., Simonson, T., and Warren, G.L. (1998) Crystallography and NMR system: a new software suite for macromolecular structure determination. *Acta Crystallogr.* **D54**, 905–921
22. Navana, J. (1994) AMoRe: an automated package for molecular replacement. *Acta Crystallogr. Sect. A*, **50**, 157–163
23. Luzatti, V. (1952) Traitement statistique des erreurs dans la determination des structures cristallines. *Acta Crystallogr. Sect. A*, **5**, 802–810
24. Ramachandran, G.N. and Sasisekharan, V. (1968) Conformation of polypeptides and proteins. *Adv. Protein Chem.* **23**, 283–437
25. Nakayama, T., Esaki, N., Tanaka, H., and Soda, K. (1988) Chemical modification of cysteine residues of L-methionine γ-lyase. *Agric. Biol. Chem.* **52**, 177–183
26. Inoue, H., Inagaki, K., Adachi, N., Tamura, T., Esaki, N., Soda, K., and Tanaka, H. (2000) Role of tyrosine 114 of L-methionine γ-lyase from *Pseudomonas putida*. *Biosci. Biotechnol. Biochem.* **64**, in press
27. Barton, G.J. (1993) ALSCRIPT a tool to format multiple sequence alignments. *Protein Eng.* **6**, 37–40